

Solution of arbitrarily dimensional matrix equation in computational electromagnetics by fast lifting wavelet-like transform

Ming-Sheng Chen^{1,*}, Wei Sha² and Xian-Liang Wu¹

¹*Department of Physics and Electronic Engineering, Hefei Teachers College, 327 Jinzhai Road, Hefei 230061, China*

²*Department of Electrical and Electronic Engineering, The University of Hong Kong, Pokfulam Road, Hong Kong, China*

SUMMARY

A new wavelet matrix transform (WMT), operated by lifting wavelet-like transform (LWLT), is applied to the solution of matrix equations in computational electromagnetics. The method can speedup the WMT without allocating auxiliary memory for transform matrices and can be implemented with the absence of the fast Fourier transform. Furthermore, to handle the matrix equation of arbitrarily dimension, a new in-space preprocessing technique based on LWLT is constructed to eliminate the limitation in matrix dimension. Complexity analysis and numerical simulation show the superiority of the proposed algorithm in saving CPU time. Numerical simulations for scattering analysis of differently shaped objects are considered to validate the effectiveness of the proposed method. In particular, due to its generality, the proposed preprocessing technique can be extended to other engineering areas and therefore can pave a broad way for the application of the WMT. Copyright © 2009 John Wiley & Sons, Ltd.

Received 17 September 2008; Revised 3 May 2009; Accepted 14 May 2009

KEY WORDS: wavelet matrix transform; method of moments; arbitrary dimension wavelet matrix transform method; lifting wavelet-like transform

1. INTRODUCTION

The method of moments (MOM) has been widely used to solve integral equations arising in electromagnetic (EM) scattering problems [1–3], and the integral equation algorithms are very

*Correspondence to: Ming-Sheng Chen, Department of Physics and Electronic Engineering, Hefei Teachers College, 327 Jinzhai Road, Hefei 230061, China.

†E-mail: cms@ahu.edu.cn

Contract/grant sponsor: Anhui Provincial Natural Science Foundation; contract/grant number: 090412047
Contract/grant sponsor: Natural Science Foundation of the Anhui Higher Education Institution of China; contract/grant number: KJ2008A036

Contract/grant sponsor: National Natural Science Foundation of China; contract/grant number: 60671051

convenient for solving the unbounded EM scattering problems with high accuracy [4], since the radiation boundary conditions are satisfied automatically. However, the impedance matrix generated by MOM is always a dense matrix, which often becomes computationally expensive and memory consuming, especially when the electrical size of the object becomes large [5]. To overcome this difficulty, various algorithms have been developed during the past decades, such as the fast multipole method [6–10], the adaptive integral equation method [11], the conjugate gradient-fast Fourier transform algorithm [12, 13], and the wavelet transform method [14–16].

Generally, wavelets have been applied to the solution of integral equations in two ways. One is to be used directly as basis functions and test functions in MOM, including periodic wavelets and intervallic wavelets, etc., which are introduced in [17, 18]. However, this approach requires considerable computational work to evaluate the complex integrals. The other is to generate the impedance matrix by MOM using conventional basis and testing functions, and then the discrete wavelet transform (DWT) is applied to the impedance matrix to obtain a sparse matrix equation in wavelet domain [19–21]. The computational cost is substantially reduced by implementing the wavelet matrix transform (WMT) and a great amount of research papers about DWT have been published by EM researchers. Unfortunately, the application of such WMT is always limited to the matrix equation with the dimension of $2^n \times 2^n$ [22–25]. To satisfy this dimension condition, only problems of special electrical size can be solved; otherwise, the number of unknowns in the discretized integral equation is usually increased intentionally, which will result in additional computational operations. Especially for three-dimensional (3-D) scattering problems, one can hardly get a suitable number of unknowns.

In this paper, the improved lifting wavelet-like transform (LWLT) scheme is proposed to alleviate this problem. The wavelet transform implemented by lifting algorithm presents an in-space matrix transform method, which can speedup the transform by a factor of two without allocating memory for constructing a wavelet transform matrix. Meanwhile, an arbitrarily dimensional technique is proposed to complete the matrix transform properly.

2. THEORY

2.1. The fast lifting scheme for wavelet transform

As shown in Figure 1, a wavelet transform can be performed by a filter bank. The forward transform uses a low-pass filter \tilde{h} and a high-pass filter \tilde{g} followed by subsampling. The inverse transform is constructed by first performing an upsampling and then using two synthesis filters h and g .

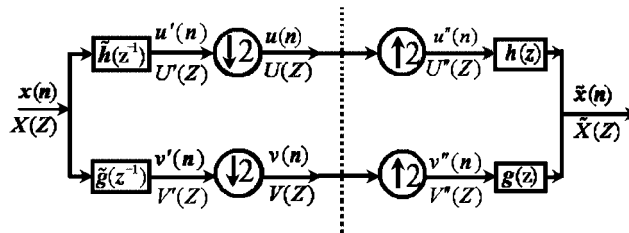


Figure 1. The structure of the discrete wavelet transform.

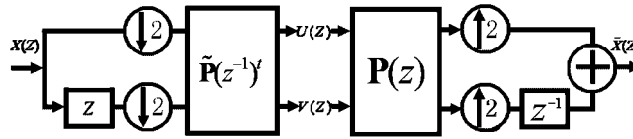


Figure 2. The polyphase matrices representation of wavelet transform.

To describe the special structure of the lifting scheme, the polyphase representation of a filter F is introduced as

$$F(z) = F_e(z^2) + z^{-1}F_o(z^2), \quad F = h, g, \tilde{h}, \tilde{g} \tag{1}$$

in which e and o denote even component and odd component of the filters, respectively

$$F_e(z) = \sum_k F_{2k}z^{-k}, \quad F_o(z) = \sum_k F_{2k+1}z^{-k} \tag{2}$$

$$F_e(z^2) = \frac{F(z) + F(-z)}{2}, \quad F_o(z^2) = \frac{F(z) - F(-z)}{2z^{-1}} \tag{3}$$

The polyphase matrix is defined as

$$\mathbf{P}(z) = \begin{pmatrix} h_e(z) & g_e(z) \\ h_o(z) & g_o(z) \end{pmatrix} \tag{4}$$

the dual polyphase matrix $\tilde{\mathbf{P}}(z)$ can be defined similarly, and the forward transform shown in Figure 1 can be represented by

$$\begin{pmatrix} U(z) \\ V(z) \end{pmatrix} = \begin{pmatrix} \tilde{h}_e(z^{-1}) & \tilde{h}_o(z^{-1}) \\ \tilde{g}_e(z^{-1}) & \tilde{g}_o(z^{-1}) \end{pmatrix} \begin{pmatrix} X_e(z) \\ X_o(z) \end{pmatrix} = \tilde{\mathbf{P}}(z^{-1})^t \begin{pmatrix} X_e(z) \\ X_o(z) \end{pmatrix} \tag{5}$$

Similarly, the inverse transform can be implemented by $\mathbf{P}(z)$. As shown in Figure 2, the forward transform in traditional DWT can be completed by subsampling even and odd samples followed by the application of dual polyphase matrix, whereas the inverse transform first uses the polyphase matrix and then an upsampling is applied. As can be seen from Figure 2, the information of both the forward transform and the inverse transform is included in the polyphase matrix and its dual matrix.

2.2. Specific steps for lifting wavelet-like matrix transform

Solved by MOM, the EM integral equation can always be reduced to a matrix equation by

$$\mathbf{Z}\mathbf{I} = \mathbf{V} \tag{6}$$

where \mathbf{Z} is the impedance matrix with size N , \mathbf{I} is the unknown current coefficients vector, and \mathbf{V} is the excitation vector.

By a WMT method, Equation (6) is transformed as

$$\tilde{\mathbf{W}}\mathbf{Z}\mathbf{W}\tilde{\mathbf{W}}\mathbf{I} = \tilde{\mathbf{W}}\mathbf{V} \tag{7}$$

where $\tilde{\mathbf{W}}$ and \mathbf{W} are assumed to be $N \times N$ matrices with identity $\mathbf{W}\tilde{\mathbf{W}} = \tilde{\mathbf{W}}\mathbf{W} = \mathbf{U}$, and for orthogonal wavelets, $\mathbf{W} = \tilde{\mathbf{W}}^t$. Set $\tilde{\mathbf{Z}} = \tilde{\mathbf{W}}\mathbf{Z}\mathbf{W}$, $\tilde{\mathbf{I}} = \tilde{\mathbf{W}}\mathbf{I}$, and $\tilde{\mathbf{V}} = \tilde{\mathbf{W}}\mathbf{V}$, one can get

$$\tilde{\mathbf{Z}}\tilde{\mathbf{I}} = \tilde{\mathbf{V}} \tag{8}$$

Then a threshold is applied to the elements of $\tilde{\mathbf{Z}}$ to eliminate the small values to make it sparse.

The WMT shown in Equation (8) has attracted a great deal of attention in computational EM field since it can greatly speedup the matrix-vector multiplication (MVM).

However, there are also some inherent pitfalls with the method mentioned above. On the one hand, auxiliary memory must be allocated for transform matrices $\tilde{\mathbf{W}}$ and \mathbf{W} . On the other hand, owing to the construction of transform matrices, the dimension of the matrix to be transformed is always limited to $2^n \times 2^n$, which seriously impede the application of this method. For example, the total number of unknowns is increased intentionally to be 4096, though 2901 unknowns are efficient for solving a specific problem.

In this section, the first pitfall is eliminated by the fast LWLT. And the second one will be described and alleviated in the next section.

Daubechies and Sweldens have proved in [26] that given a complementary filter pair $\{h, g\}$ or $\{\tilde{h}, \tilde{g}\}$, then there always exist Laurent polynomials $s_i(z)$ and $t_i(z)$ for $1 \leq i \leq m$ and a nonzero constant K so that

$$\mathbf{P}(z) = \prod_{i=1}^m \begin{pmatrix} 1 & s_i(z) \\ 0 & 1 \end{pmatrix} \begin{pmatrix} 1 & 0 \\ t_i(z) & 1 \end{pmatrix} \begin{pmatrix} K & 0 \\ 0 & \frac{1}{K} \end{pmatrix} \tag{9}$$

$$\tilde{\mathbf{P}}(z) = \prod_{i=1}^m \begin{pmatrix} 1 & 0 \\ -s_i(z^{-1}) & 1 \end{pmatrix} \begin{pmatrix} 1 & -t_i(z^{-1}) \\ 0 & 1 \end{pmatrix} \begin{pmatrix} K & 0 \\ 0 & \frac{1}{K} \end{pmatrix} \tag{10}$$

Without loss of generality, we take the db2 wavelet, for example, to illuminate the specific steps to implement the WMT by lifting wavelet-like scheme. The filters \tilde{h} and \tilde{g} for it are defined as

$$\tilde{h}(z^{-1}) = h_0 + h_1z^{-1} + h_2z^{-2} + h_3z^{-3} \tag{11}$$

$$\tilde{g}(z^{-1}) = -h_3z^2 + h_2z^1 - h_1 + h_0z^{-1} \tag{12}$$

in which

$$h_0 = \frac{1 + \sqrt{3}}{4\sqrt{2}}, \quad h_1 = \frac{3 + \sqrt{3}}{4\sqrt{2}}, \quad h_2 = \frac{3 - \sqrt{3}}{4\sqrt{2}}, \quad h_3 = \frac{1 - \sqrt{3}}{4\sqrt{2}}$$

From the definition of polyphase matrix and its dual matrix, one can obtain

$$\tilde{\mathbf{P}}(z^{-1}) = \begin{pmatrix} \tilde{h}_e(z^{-1}) & \tilde{g}_e(z^{-1}) \\ \tilde{h}_o(z^{-1}) & \tilde{g}_o(z^{-1}) \end{pmatrix} = \begin{bmatrix} h_0 + h_2z^{-1} & -h_3z^1 - h_1 \\ h_1 + h_3z^{-1} & h_2z^1 + h_0 \end{bmatrix} \tag{13}$$

which can be factored as the product of matrices of the form

$$\tilde{\mathbf{P}}(z^{-1}) = \begin{bmatrix} 1 & -\sqrt{3} \\ 0 & 1 \end{bmatrix} \begin{bmatrix} 1 & 0 \\ \frac{\sqrt{3}}{4} + \frac{\sqrt{3}-2}{4}z^{-1} & 1 \end{bmatrix} \begin{bmatrix} 1 & z \\ 0 & 1 \end{bmatrix} \begin{bmatrix} \frac{\sqrt{3}+1}{\sqrt{2}} & 0 \\ 0 & \frac{\sqrt{3}-1}{\sqrt{2}} \end{bmatrix} \quad (14)$$

and the transpose of it is given by

$$\tilde{\mathbf{P}}(z^{-1})^t = \begin{bmatrix} \frac{\sqrt{3}+1}{\sqrt{2}} & 0 \\ 0 & \frac{\sqrt{3}-1}{\sqrt{2}} \end{bmatrix} \begin{bmatrix} 1 & 0 \\ z & 1 \end{bmatrix} \begin{bmatrix} 1 & \frac{\sqrt{3}}{4} + \frac{\sqrt{3}-2}{4}z^{-1} \\ 0 & 1 \end{bmatrix} \begin{bmatrix} 1 & 0 \\ -\sqrt{3} & 1 \end{bmatrix} \quad (15)$$

Obviously, $\mathbf{P}(z)$ can be computed from the (perfect reconstruction) PR conditions as

$$\begin{aligned} \mathbf{P}(z) &= (\tilde{\mathbf{P}}(z^{-1})^t)^{-1} \\ &= \begin{bmatrix} 1 & 0 \\ \sqrt{3} & 1 \end{bmatrix} \begin{bmatrix} 1 & -\frac{\sqrt{3}}{4} - \frac{\sqrt{3}-2}{4}z^{-1} \\ 0 & 1 \end{bmatrix} \begin{bmatrix} 1 & 0 \\ -z & 1 \end{bmatrix} \begin{bmatrix} \frac{\sqrt{3}-1}{\sqrt{2}} & 0 \\ 0 & \frac{\sqrt{3}+1}{\sqrt{2}} \end{bmatrix} \end{aligned} \quad (16)$$

$$\mathbf{P}(z^{-1})^t = \begin{bmatrix} \frac{\sqrt{3}-1}{\sqrt{2}} & 0 \\ 0 & \frac{\sqrt{3}+1}{\sqrt{2}} \end{bmatrix} \begin{bmatrix} 1 & -z^{-1} \\ 0 & 1 \end{bmatrix} \begin{bmatrix} 1 & 0 \\ -\frac{\sqrt{3}}{4} - \frac{\sqrt{3}-2}{4}z & 1 \end{bmatrix} \begin{bmatrix} 1 & \sqrt{3} \\ 0 & 1 \end{bmatrix} \quad (17)$$

According to the structure shown in Figure 2 and Equation (5), and with the help of the factorization of $\tilde{\mathbf{P}}(z^{-1})^t$ in Equation (15), we can get the following implementations for the forward transform:

$$\mathbf{x}_e(l) = \mathbf{x}(2l) \quad (18a)$$

$$\mathbf{x}_o(l) = \mathbf{x}(2l+1) \quad (18b)$$

$$\mathbf{x}_e^{(1)}(l) = \mathbf{x}_e(l) \quad (19a)$$

$$\mathbf{x}_o^{(1)}(l) = \mathbf{x}_o(l) - \sqrt{3}\mathbf{x}_e(l) \quad (19b)$$

$$\mathbf{x}_e^{(2)}(l) = \mathbf{x}_e^{(1)}(l) + \frac{\sqrt{3}}{4}\mathbf{x}_o^{(1)}(l) + \frac{\sqrt{3}-2}{4}\mathbf{x}_o^{(1)}(l+1) \quad (20a)$$

$$\mathbf{x}_o^{(2)}(l) = \mathbf{x}_o^{(1)}(l) \quad (20b)$$

$$\mathbf{x}_e^{(3)}(l) = \mathbf{x}_e^{(2)}(l) \quad (21a)$$

$$\mathbf{x}_o^{(3)}(l) = \mathbf{x}_o^{(2)}(l) + \mathbf{x}_e^{(2)}(l-1) \quad (21b)$$

$$\tilde{\mathbf{x}}_e = \mathbf{x}_e^{(4)}(l) = \frac{\sqrt{3}+1}{\sqrt{2}} \mathbf{x}_e^{(3)}(l) \tag{22a}$$

$$\tilde{\mathbf{x}}_o = \mathbf{x}_o^{(4)}(l) = \frac{\sqrt{3}-1}{\sqrt{2}} \mathbf{x}_o^{(3)}(l) \tag{22b}$$

And for the impedance matrix, the left-hand forward transform (for the impedance matrix $\hat{\mathbf{Z}} = \tilde{\mathbf{W}}\mathbf{Z}$, for the vector transform $\tilde{\mathbf{I}} = \tilde{\mathbf{W}}\mathbf{I}$ or $\tilde{\mathbf{V}} = \tilde{\mathbf{W}}\mathbf{V}$) will be performed by the following implementation steps:

$$\hat{\mathbf{Z}}^{(0)} \left(\left[1 : \frac{N}{2} \right], \cdot \right) = \mathbf{Z}([2:2:N], \cdot) \tag{23a}$$

$$\hat{\mathbf{Z}}^{(0)} \left(\left[\frac{N}{2} + 1 : N \right], \cdot \right) = \mathbf{Z}([1:2:N-1], \cdot) \tag{23b}$$

$$\hat{\mathbf{Z}}^{(1)} \left(\left[1 : \frac{N}{2} \right], \cdot \right) = \hat{\mathbf{Z}}^{(0)} \left(\left[1 : \frac{N}{2} \right], \cdot \right) \tag{24a}$$

$$\hat{\mathbf{Z}}^{(1)} \left(\left[\frac{N}{2} + 1 : N \right], \cdot \right) = \hat{\mathbf{Z}}^{(0)} \left(\left[\frac{N}{2} + 1 : N \right], \cdot \right) - \sqrt{3} \times \hat{\mathbf{Z}}^{(0)} \left(\left[1 : \frac{N}{2} \right], \cdot \right) \tag{24b}$$

$$\hat{\mathbf{Z}}^{(2)}(1, \cdot) = \hat{\mathbf{Z}}^{(1)}(1, \cdot) + \frac{\sqrt{3}}{4} \hat{\mathbf{Z}}^{(1)} \left(\frac{N}{2} + 1, \cdot \right) + \frac{\sqrt{3}-2}{4} \hat{\mathbf{Z}}^{(1)}(N, \cdot) \tag{25a}$$

$$\begin{aligned} \hat{\mathbf{Z}}^{(2)} \left(\left[2 : \frac{N}{2} \right], \cdot \right) &= \hat{\mathbf{Z}}^{(1)} \left(\left[2 : \frac{N}{2} \right], \cdot \right) + \frac{\sqrt{3}}{4} \hat{\mathbf{Z}}^{(1)} \left(\left[\frac{N}{2} + 2 : N \right], \cdot \right) \\ &+ \frac{\sqrt{3}-2}{4} \hat{\mathbf{Z}}^{(1)} \left(\left[\frac{N}{2} + 1 : N - 1 \right], \cdot \right) \end{aligned} \tag{25b}$$

$$\hat{\mathbf{Z}}^{(2)} \left(\left[\frac{N}{2} + 1 : N \right], \cdot \right) = \hat{\mathbf{Z}}^{(1)} \left(\left[\frac{N}{2} + 1 : N \right], \cdot \right) \tag{25c}$$

$$\hat{\mathbf{Z}}^{(3)} \left(\left[1 : \frac{N}{2} \right], \cdot \right) = \hat{\mathbf{Z}}^{(2)} \left(\left[1 : \frac{N}{2} \right], \cdot \right) \tag{26a}$$

$$\hat{\mathbf{Z}}^{(3)}(N, \cdot) = \hat{\mathbf{Z}}^{(2)}(N, \cdot) + \hat{\mathbf{Z}}^{(3)}(1, \cdot) \tag{26b}$$

$$\hat{\mathbf{Z}}^{(3)} \left(\left[\frac{N}{2} + 1 : N - 1 \right], \cdot \right) = \hat{\mathbf{Z}}^{(2)} \left(\left[\frac{N}{2} + 1 : N - 1 \right], \cdot \right) + \hat{\mathbf{Z}}^{(3)} \left(\left[2 : \frac{N}{2} \right], \cdot \right) \tag{26c}$$

$$\hat{\mathbf{Z}}^{(4)} \left(\left[1 : \frac{N}{2} \right], \cdot \right) = \frac{\sqrt{3}+1}{\sqrt{2}} \hat{\mathbf{Z}}^{(3)} \left(\left[1 : \frac{N}{2} \right], \cdot \right) \tag{27a}$$

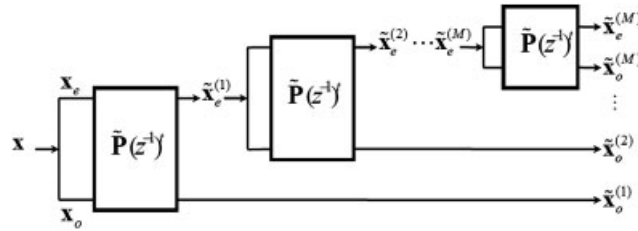


Figure 3. The global structure for multilevel forward transform.

$$\hat{\mathbf{Z}}^{(4)} \left(\left[\frac{N}{2} + 1 : N \right], \cdot \right) = \frac{\sqrt{3}-1}{\sqrt{2}} \hat{\mathbf{Z}}^{(3)} \left(\left[\frac{N}{2} + 1 : N \right], \cdot \right) \tag{27b}$$

$$\hat{\mathbf{Z}} = \hat{\mathbf{Z}}^{(4)} \tag{28}$$

in the above equations, N is the dimension of matrix \mathbf{Z} , the periodic extension is applied in (25a) and (26b).

To complete multilevel forward transform by lifting scheme, one just needs to replace N with $N^{(i)} = N/2^i$ ($i = 0, 1, 2, \dots$) and repeat the operations according to Equations (23)–(28) until the $N^{(M)} = N/2^M$ is not a integer or $N^{(M)}$ is small enough (the transforms for $N^{(M)} \leq 16$ are ignored in this paper). Finally, to illustrate the operations for multilevel forward transform, a global structure is described in Figure 3.

The right-hand forward transform $\tilde{\mathbf{Z}} = \hat{\mathbf{Z}}\mathbf{W}$ can be operated by the factorization of $\mathbf{P}(z^{-1})^t$, which is the dual matrix of $\tilde{\mathbf{P}}(z^{-1})^t$. The specific steps are similar to Equations (23)–(28) and are neglected here for the sake of brevity. In the orthonormal wavelet case, $\mathbf{P}(z) = \tilde{\mathbf{P}}(z)$, $\mathbf{P}(z^{-1})^t = \tilde{\mathbf{P}}(z^{-1})^t$, and $\mathbf{W} = \tilde{\mathbf{W}}^{-1} = \tilde{\mathbf{W}}^t$. The right-hand forward transform $\tilde{\mathbf{Z}} = \hat{\mathbf{Z}}$ can also be completed by transposing $\hat{\mathbf{Z}}$ firstly and then operating the transform to $\hat{\mathbf{Z}}^t$ by Equations (23)–(28).

Similarly, the inverse transform $\mathbf{I} = \tilde{\mathbf{W}}^{-1}\hat{\mathbf{I}} = \mathbf{W}\hat{\mathbf{I}}$ is operated by the factorization of $\mathbf{P}(z)$ in Equation (16).

$$\mathbf{I}^{(0)} \left(1 : \frac{N}{2} \right) = \frac{\sqrt{3}-1}{\sqrt{2}} \hat{\mathbf{I}} \left(1 : \frac{N}{2} \right) \tag{29a}$$

$$\mathbf{I}^{(0)} \left(\frac{N}{2} + 1 : N \right) = \frac{\sqrt{3}+1}{\sqrt{2}} \hat{\mathbf{I}} \left(\frac{N}{2} + 1 : N \right) \tag{29b}$$

$$\mathbf{I}^{(1)} \left(1 : \frac{N}{2} \right) = \mathbf{I}^{(0)} \left(1 : \frac{N}{2} \right) \tag{30a}$$

$$\mathbf{I}^{(1)} \left(\frac{N}{2} + 1 : N - 1 \right) = \mathbf{I}^{(0)} \left(\frac{N}{2} + 1 : N - 1 \right) - \mathbf{I}^{(0)} \left(2 : \frac{N}{2} \right) \tag{30b}$$

$$\mathbf{I}^{(1)}(N) = \mathbf{I}^{(0)}(N) - \mathbf{I}^{(0)}(1) \tag{30c}$$

$$\mathbf{I}^{(2)}(1) = \mathbf{I}^{(1)}(1) - \frac{\sqrt{3}}{4}\mathbf{I}^{(1)}\left(\frac{N}{2} + 1\right) - \frac{\sqrt{3}-2}{4}\mathbf{I}^{(2)}(N) \quad (31a)$$

$$\mathbf{I}^{(2)}\left(2:\frac{N}{2}\right) = \mathbf{I}^{(1)}\left(2:\frac{N}{2}\right) - \frac{\sqrt{3}}{4}\mathbf{I}^{(2)}\left(\frac{N}{2} + 2:N\right) - \frac{\sqrt{3}-2}{4}\mathbf{I}^{(2)}\left(\frac{N}{2} + 1:N-1\right) \quad (31b)$$

$$\mathbf{I}^{(2)}\left(\frac{N}{2} + 1:N\right) = \mathbf{I}^{(1)}\left(\frac{N}{2} + 1:N\right) \quad (31c)$$

$$\mathbf{I}^{(3)}\left(1:\frac{N}{2}\right) = \mathbf{I}^{(2)}\left(1:\frac{N}{2}\right) \quad (32a)$$

$$\mathbf{I}^{(3)}\left(\frac{N}{2} + 1:N\right) = \mathbf{I}^{(2)}\left(\frac{N}{2} + 1:N\right) + \sqrt{3}\mathbf{I}^{(2)}\left(1:\frac{N}{2}\right) \quad (32b)$$

$$\mathbf{I}(1:2:N-1) = \mathbf{I}^{(3)}\left(\frac{N}{2} + 1:N\right) \quad (33a)$$

$$\mathbf{I}(2:2:N) = \mathbf{I}^{(3)}\left(1:\frac{N}{2}\right) \quad (33b)$$

the periodic extension is applied in (30c) and (31a).

To complete the corresponding multilevel inverse transform by lifting scheme, one just needs to replace N with $N^{(M-i)} = N/2^{M-i}$ ($i = 1, 2, \dots, M$) and repeat the operations according to Equations (29)–(33).

The physical meaning of the scheme is given below. For simplicity, we take the lifting scheme of Harr wavelet for example, where we ignore the final step for orthogonality.

$$\mathbf{x}_o(l) = \mathbf{x}(2l+1)$$

$$\mathbf{x}_e(l) = \mathbf{x}(2l)$$

$$\tilde{\mathbf{x}}_o(l) = \mathbf{x}_o(l) - \mathbf{x}_e(l)$$

$$\tilde{\mathbf{x}}_e(l) = \mathbf{x}_e(l) + 0.5 \cdot \tilde{\mathbf{x}}_o(l)$$

The fluctuation term $\tilde{\mathbf{x}}_o$, which contains the minor information of the impedance matrix, can be predicted by the difference of the odd and even components. The leading term $\tilde{\mathbf{x}}_e$, which contains the major information and properties (mean, high-order moments, etc.) of the impedance matrix, can be updated by the fluctuation term and the even component. The fluctuation of the impedance matrix element leads to the fluctuation of currents. The noise-like current fluctuation is expected to be very small and random, so that it plays little contribution for far-field computation. Based on the explanation, we can set the fluctuation term $\tilde{\mathbf{x}}_o$ to be zero, and we can also decompose the leading term $\tilde{\mathbf{x}}_e$ again by the multilevel implementation.

Table I. The complexity comparison for $\hat{\mathbf{Z}} = \tilde{\mathbf{W}}\mathbf{Z}$.

Wavelet type	Haar	db2	db4	db6	db8	CDF9/7
Wavelet-like transform	$4N^2$	$8N^2$	$16N^2$	$24N^2$	$32N^2$	$16N^2$
Lifting wavelet-like transform	$3N^2$	$5N^2$	$12N^2$	$14N^2$	$20N^2$	$6N^2$

Table II. CPU time for wavelet matrix transform (units: seconds).

Wavelet type	db4		db8		CDF9/7	
	$N = 2048$	$N = 4096$	$N = 2048$	$N = 4096$	$N = 2048$	$N = 4096$
Wavelet-like transform	2.47	9.21	4.71	18.9	2.39	9.07
Lifting wavelet-like transform	1.71	6.83	2.84	11.3	0.90	3.44

2.3. Computational complexity and CPU time comparison

The computation complexity evaluation for the wavelet-like transforms used for preprocessing a matrix is now investigated. The 1-D wavelet transform of a vector can be completed by a number of multiplications given by

$$qN \times \left(1 + \frac{1}{2} + \frac{1}{4} + \dots\right) = 2qN \quad (34)$$

where q is the length of the filter, N is the size of the vector. For an $N \times N$ matrix the total complexity for $\hat{\mathbf{Z}} = \tilde{\mathbf{W}}\mathbf{Z}$ will be described by $2qN^2$.

The number of operations for the LWLT scheme is

$$p \frac{N}{2} \left(1 + \frac{1}{2} + \frac{1}{4} + \dots\right) = pN \quad (35)$$

where p is the number of multiplications included in the polyphase matrix. For an $N \times N$ matrix the total complexity for $\hat{\mathbf{Z}} = \tilde{\mathbf{W}}\mathbf{Z}$ will be computed by pN^2 .

The complexity of the operation for $\hat{\mathbf{Z}} = \tilde{\mathbf{W}}\mathbf{Z}$ by several kinds of wavelet is shown in Table I, and the comparison of CPU time consumed for WMT is illuminated in Table II. From this we can conclude that the LWLT scheme is faster than the wavelet-like transform, especially for the wavelet with high vanishing moments and biorthogonal wavelet such as Cohen Daubechies Feauveau 9/7 (CDF9/7), since the factorization of polyphase matrix for wavelet with high vanishing moments can be optimized and the multiplications in CDF9/7 can be merged by distributive law.

In addition, the reason why the lifting scheme is faster than the traditional wavelet-like transform can be traced to a classic mathematical method. For example, a polynomial $f(x) = x^3 - 6x^2 + 11x - 6$ can be factorized into a nested representation $f(x) = 6 + (11 + (-6 + x)x)x$.

2.4. Algorithm for solution of arbitrarily dimensional matrix equation

To alleviate the limitation in the dimension of impedance matrix \mathbf{Z} , a novel method in conjugation with the LWLT is proposed in this section.

From the specific steps for lifting wavelet-like matrix transform described in the previous section, we can see that the LWLT comes to a standstill at the M th level when $N^{(M)}$ cannot be divided by 2. For the sake of convenience, we describe the zeroth-level LWLT for matrix \mathbf{Z} (LWLTM) as

$$\tilde{\mathbf{Z}}^{(0)} = \text{LWLTM}^{(0)}(\mathbf{Z}) \tag{36a}$$

the zeroth-level LWLT for vector \mathbf{I} or \mathbf{V} (LWLTV) is given as

$$\tilde{\mathbf{I}}^{(0)} = \text{LWLTV}^{(0)}(\mathbf{I}), \quad \tilde{\mathbf{V}}^{(0)} = \text{LWLTV}^{(0)}(\mathbf{V}) \tag{36b}$$

Then the matrix equation in Equation (6) is transformed to be

$$\tilde{\mathbf{Z}}^{(0)}\tilde{\mathbf{I}}^{(0)} = \tilde{\mathbf{V}}^{(0)} \tag{36c}$$

and \mathbf{I} will be solved by the inverse LWLT transform (ILWLT)

$$\mathbf{I} = \text{ILWLT}^{(0)}(\tilde{\mathbf{I}}^{(0)}) \tag{36d}$$

Generally, the matrix equation after $i - 1$ th-level LWLT is given by

$$\tilde{\mathbf{Z}}^{(i-1)}\tilde{\mathbf{I}}^{(i-1)} = \tilde{\mathbf{V}}^{(i-1)} \tag{37}$$

the i th-level LWLT will be given as

$$\tilde{\mathbf{Z}}^{(i)} = \text{LWLTM}^{(i)}(\tilde{\mathbf{Z}}^{(i-1)}) \tag{38a}$$

$$\tilde{\mathbf{I}}^{(i)} = \text{LWLTV}^{(i)}(\tilde{\mathbf{I}}^{(i-1)}), \quad \tilde{\mathbf{V}}^{(i)} = \text{LWLTV}^{(i)}(\tilde{\mathbf{V}}^{(i-1)}) \tag{38b}$$

and the matrix equation in Equation (6) is transformed to be

$$\tilde{\mathbf{Z}}^{(i)}\tilde{\mathbf{I}}^{(i)} = \tilde{\mathbf{V}}^{(i)} \tag{38c}$$

$\tilde{\mathbf{I}}^{(i-1)}$ will be obtained by

$$\tilde{\mathbf{I}}^{(i-1)} = \text{ILWLT}^{(i)}(\tilde{\mathbf{I}}^{(i)}) \tag{38d}$$

When $N^{(i)}/2$ is not a integer, the $i + 1$ th-level LWLT cannot be carried out any further. To handle the $i + 1$ th-level LWLT, we introduce a new matrix

$$\tilde{\mathbf{Z}}^{(i)} = \begin{pmatrix} \alpha\mathbf{\Lambda}_{m \times m} & \mathbf{0} \\ \mathbf{0} & \tilde{\mathbf{Z}}^{(i)} \end{pmatrix} \tag{39a}$$

$$\tilde{\mathbf{V}}^{(i)} = \begin{pmatrix} \beta\mathbf{\Gamma}_{m \times 1} \\ \tilde{\mathbf{V}}^{(i)} \end{pmatrix} \tag{39b}$$

$$\mathbf{\Lambda}_{m \times m} = \begin{pmatrix} 1 & & & \\ & 1 & & \\ & & \ddots & \\ & & & 1 \end{pmatrix}_{m \times m}, \quad \mathbf{\Gamma}_{m \times 1} = \begin{pmatrix} 1 \\ 1 \\ \vdots \\ 1 \end{pmatrix}_{m \times 1} \tag{39c}$$

The integer m is an odd number and usually chosen to be 1. To make the condition number unchanged and to avoid the truncation error, α and β are always computed by

$$\alpha = \text{trace}(\tilde{\mathbf{Z}}^{(i)})/N \tag{39d}$$

$$\beta = \text{mean}(\tilde{\mathbf{V}}^{(i)}) \tag{39e}$$

Then the matrix equation will be given by

$$\tilde{\mathbf{Z}}^{(i)}\tilde{\mathbf{I}}^{(i)} = \tilde{\mathbf{V}}^{(i)} \tag{39f}$$

Obviously, $\tilde{\mathbf{I}}^{(i)}$ is included in $\tilde{\mathbf{I}}^{(i)}$, and can be obtained by deleting the first element in $\tilde{\mathbf{I}}^{(i)}$.

By applying the LWLT to the new equation in (39f), the $i + 1$ th-level LWLT can be written as

$$\tilde{\mathbf{Z}}^{(i+1)}\tilde{\mathbf{I}}^{(i+1)} = \tilde{\mathbf{V}}^{(i+1)} \tag{40a}$$

$$\tilde{\mathbf{Z}}^{(i+1)} = \text{LWLTM}^{(i+1)}(\tilde{\mathbf{Z}}^{(i)}) \tag{40b}$$

$$\tilde{\mathbf{V}}^{(i+1)} = \text{LWLTV}^{(i+1)}(\tilde{\mathbf{V}}^{(i)}) \tag{40c}$$

when $\tilde{\mathbf{I}}^{(i+1)}$ is solved, $\tilde{\mathbf{I}}^{(i)}$ will be obtained by $\tilde{\mathbf{I}}^{(i)} = \text{ILWLT}^{(i+1)}(\tilde{\mathbf{I}}^{(i+1)})$. Delete the first element in $\tilde{\mathbf{I}}^{(i)}$, one will obtain $\tilde{\mathbf{I}}^{(i)}$, and \mathbf{I} will be obtained by the inverse LWLT to $\tilde{\mathbf{I}}^{(i)}$ at different levels ($\text{ILWLT}^{(i)}, \text{ILWLT}^{(i-1)}, \dots, \text{ILWLT}^{(0)}$).

The technique described above is named as ‘arbitrary dimension WMT method’, and the following theorem will be demonstrated.

Theorem

The solution of the matrix equation cannot be influenced by the application of ‘arbitrary dimension WMT method’ at different levels.

For a given matrix \mathbf{Z} , the WMT is applied to it at different levels ($\{0, 1, 2, \dots, M - 1\}$). Let $\{i_1, i_2, \dots, i_L\}$ be a subsequence of $\{0, 1, 2, \dots, M - 1\}$, at which the arbitrary dimension WMT method is applied.

$\tilde{\mathbf{I}}^{(i_L)}$ is computed by the inverse LWLT

$$\tilde{\mathbf{I}}^{(i_L)} = \text{ILWLT}^{(i_L+1)}(\tilde{\mathbf{I}}^{(i_L+1)})$$

$$\tilde{\mathbf{I}}^{(i_L+1)} = \text{ILWLT}^{(i_L+2)}(\tilde{\mathbf{I}}^{(i_L+2)})$$

⋮

$$\tilde{\mathbf{I}}^{(M-2)} = \text{ILWLT}^{(M-1)}(\tilde{\mathbf{I}}^{(M-1)})$$

$\tilde{\mathbf{I}}^{(i_L)}$ is obtained by deleting the first element in $\tilde{\mathbf{I}}^{(i_L)}$. And $\tilde{\mathbf{I}}^{(i_{L-1})}$ will be computed by

$$\tilde{\mathbf{I}}^{(i_{L-1})} = \text{ILWLT}^{(i_{L-1}+1)}(\tilde{\mathbf{I}}^{(i_{L-1}+1)})$$

$$\tilde{\mathbf{I}}^{(i_{L-1}+1)} = \text{ILWLT}^{(i_{L-1}+2)}(\tilde{\mathbf{I}}^{(i_{L-1}+2)})$$

⋮

$$\tilde{\mathbf{I}}^{(i_1)} = \text{ILWLT}^{(i_1)}(\tilde{\mathbf{I}}^{(i_1)})$$

$\tilde{\mathbf{I}}^{(i_1)}$ can be obtained by repeating the above operations, and finally \mathbf{I} is obtained.

3. NUMERICAL RESULTS

3.1. Two-dimensional examples

As the first example, an infinite perfectly electrical conducting (PEC) circular cylinder with radius of 15 wavelengths is considered. The cylinder is excited by a TM plane wave at an angle of incident $\theta_i = 0$. The surface of the circular cylinder is discretized with 1257 pulses and combined field integral equation (CFIE) is used. The Daubechies wavelet with 8 vanishing moments (db8) is adopted to operate the WMT. The arbitrary dimension WMT method is applied at the levels $\{0, 1, 2, 4\}$, which finally results into a 1261×1261 matrix shown in Figure 4. The sparsity of the wavelet-domain impedance matrix, which is defined as its percentage content of nonzero elements,

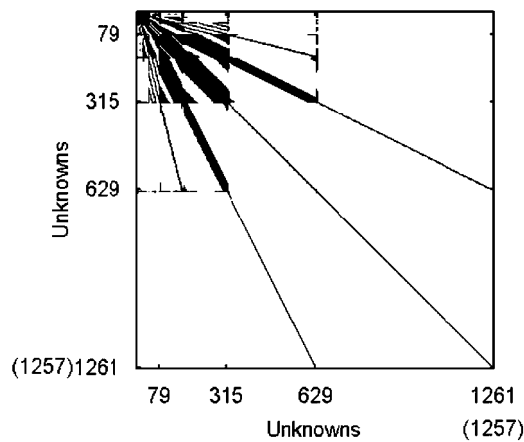


Figure 4. The wavelet-domain impedance matrix for the PEC circular cylinder.

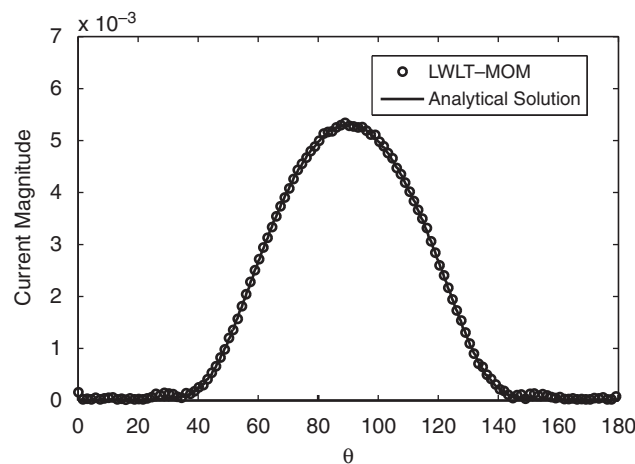


Figure 5. The surface electrical current of the PEC circular cylinder.

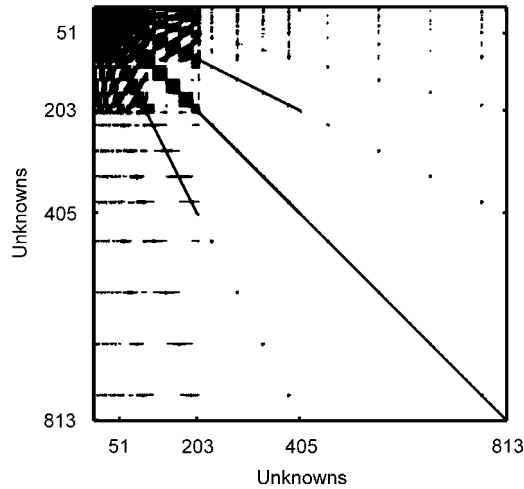


Figure 6. The wavelet-domain impedance matrix for the PEC square cylinder.

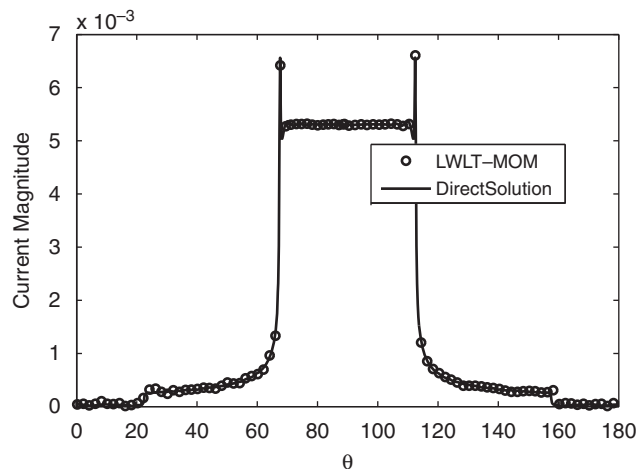


Figure 7. The surface electrical current of the PEC square cylinder.

is 4.79%, and the surface electrical current is compared with that of the analytical solution method as shown in Figure 5.

As can be seen from Figure 6, the wavelet-domain impedance matrix for an infinite PEC square cylinder with sparsity of 5.26% is presented after clipping operation. The side length of it is chosen to be $l = 11\lambda$. CFIE is used to generate the impedance matrix, and db8 wavelet is applied to get the impedance matrix in wavelet domain. The surface of the cylinder is discretized with 810 pulses, with the arbitrary dimension WMT method applied at levels $\{0, 2, 4\}$, a 813×813 wavelet-domain impedance matrix is obtained. The surface electrical current is compared with that obtained by the direct solution method as shown in Figure 7.

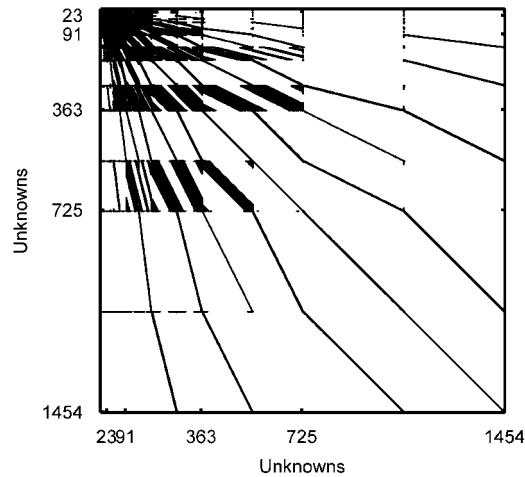


Figure 8. The wavelet-domain impedance matrix for the dielectric circular cylinder.

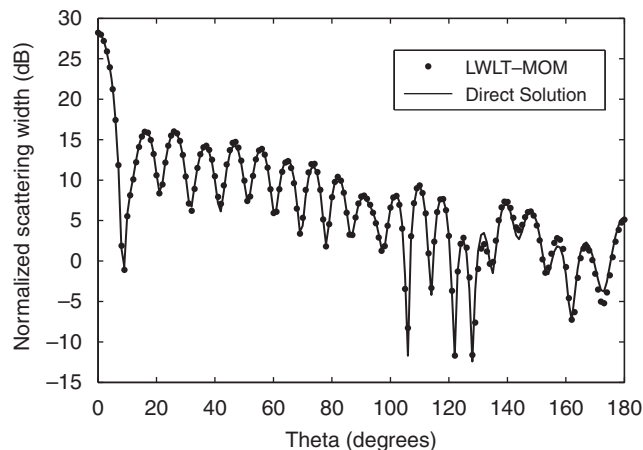


Figure 9. The normalized scattering width of the dielectric circular cylinder.

Figure 8 shows a wavelet-domain impedance matrix for a dielectric circular cylinder, the sparsity of which is 6.42%. The electrical field integral equation is solved by MOM. The object is illuminated by a TM plane wave with a frequency $f = 300$ MHz, and the parameter of it can be described as $\epsilon_r = 4$, $\mu_r = 2$, with radius of 4 m. The surface of the object is discretized with 725 pulses, which results into a 1450×1450 matrix. As the db4 wavelet is used to operate the WMT, the arbitrary dimension WMT method applied at levels $\{1, 2, 4, 6\}$, a 1454×1454 wavelet-domain impedance matrix is obtained. The normalized scattering width is computed and compared with that of the direct solution method as shown in Figure 9, and the relative root mean-square error is 1.13%.

As the final 2-D example, a composite inhomogeneous dielectric rectangular cylinder is shown in Figure 10(a). The relative permittivity of the top and bottom parts is 4 and 2, respectively.

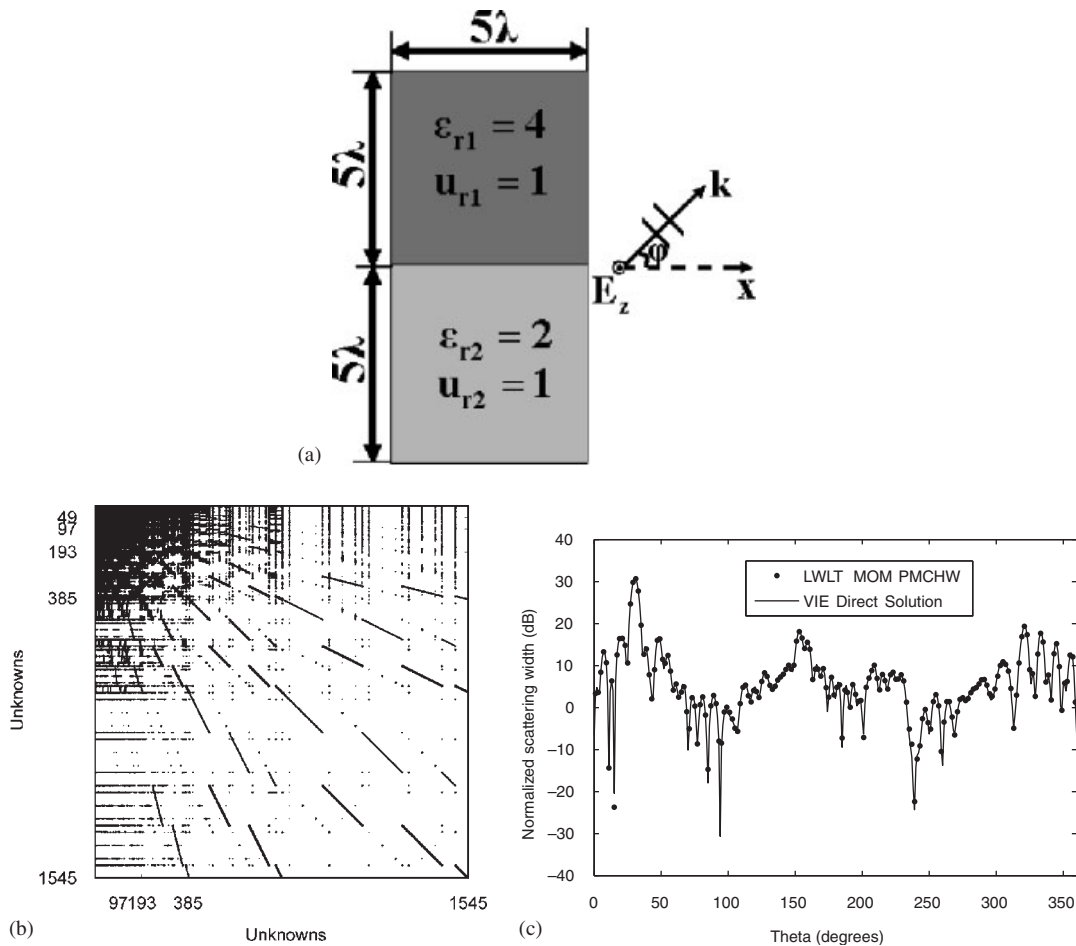


Figure 10. The scattering analysis of a composite inhomogeneous dielectric rectangular cylinder: (a) the modeling of the object; (b) the impedance matrix in wavelet-domain; and (c) the normalized scattering width of the object.

By using the LWLT scheme (db4) in conjunction with the Poggio, Miller, Chang, Harrington, and Wu (PMCHW) formulation, the normalized scattering width is computed and compared with that obtained by directly solving a volume integral equation. After the application of the arbitrary dimension WMT method at levels {2, 3, 4, 5, 6}, the dimension of the wavelet-domain impedance matrix is increased to be 1545×1545 from 1540×1540 .

3.2. 3-D examples

In Figure 11, a PEC sphere with radius of one wavelength is considered, which is illuminated by a plane wave propagating in the z direction and E-polarized in the x direction. The surface of the object is discretized into 1620 triangular elements resulting in 2430 unknown current coefficients. The bistatic radar cross section (RCS) is calculated and the result is compared with that obtained

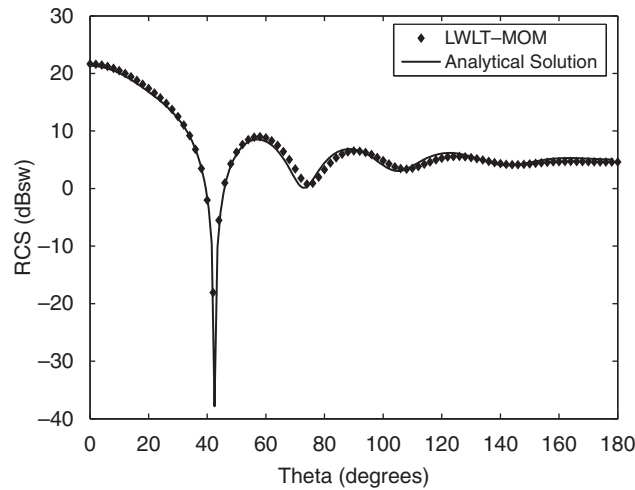


Figure 11. The E-plane RCS of a PEC sphere.

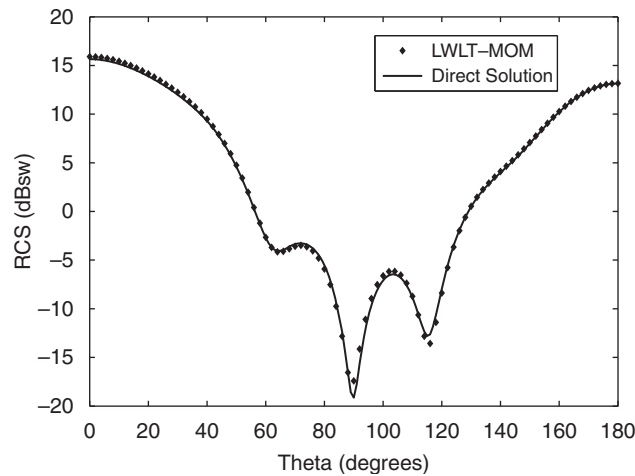


Figure 12. The E-plane RCS of a PEC cube.

by Mie series. The arbitrary dimension WMT method is applied at levels $\{1, 7\}$, which results in a 2432×2432 wavelet-domain impedance matrix.

A PEC cube with side length of 1.1λ is considered as another 3-D PEC example. With the surface discretized into 1452 triangular elements, a 2178×2178 matrix equation is generated for solution. The arbitrary dimension WMT method is applied at each level after zeroth level completed by the usual lifting WMT. As shown in Figure 12, the bistatic RCS is calculated and compared with that of the direct solution method.

In the two 3-D examples shown in Figures 11 and 12, the EFIE is built to get the solution of the surface current. To consider the effect of the proposed WMT method for the impedance matrix

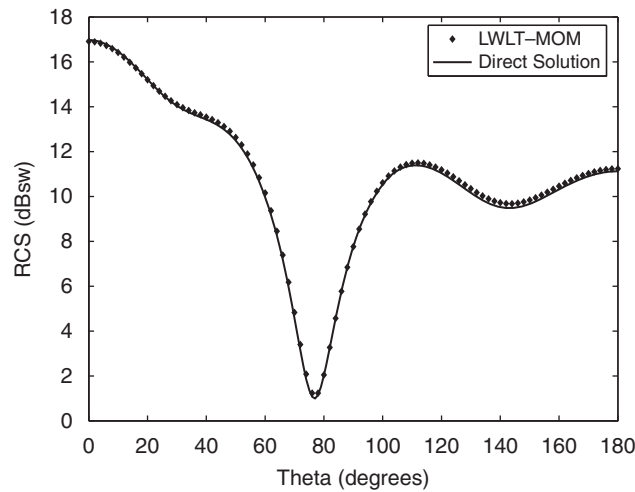


Figure 13. The E-plane RCS of a finite circular cylinder.

generated from CFIE, a finite circular cylinder is considered. The PEC circular cylinder is parallel to the y -axis with its diameter assumed to be 1λ and height to be 2λ . When it is illuminated by a plane wave propagating in the z direction and E-polarized in the x direction, the bistatic RCS is computed as shown in Figure 13. The impedance matrix generated from CFIE is a 3510×3510 matrix, which is finally transformed into a 3513×3513 wavelet-domain impedance matrix by the application of the arbitrary dimension WMT at levels $\{1, 3, 6\}$.

Finally, to validate the application of the proposed method to PMCHW equation for 3-D homogeneous dielectric objects, a homogeneous dielectric sphere with radius of 0.5 m, which is illuminated by a 300 MHz plane wave, is considered. The surface of the object is discretized into 1280 triangular elements, and the total number of the unknown currents coefficients is 3840, which makes a special example because it can be directly operated by the usual LWLT method without the use of the arbitrary dimension WMT. The relative permittivity and relative permeability are set to be $\epsilon_r = 2 - 2j$, $\mu_r = 1$. As shown in Figure 14, the E-plane RCS is computed and agrees well with that of the analytical solution.

All the computations reported above have been carried out on a Personal Computer with Pentium IV-2.66 GHz processor and 1 GB RAM. The code has been written in Microsoft Visual C++ 6.0.

When db4 is used for 3-D objects, the sparsity of the wavelet-domain impedance matrix and the CPU time consumed is shown in Table III, from which one can conclude that the proposed method can greatly speedup the MVM.

4. CONCLUSIONS

A new preprocessing technique, which is completed by LWLT method in conjunction with an arbitrarily dimension operation, is proposed to speedup the solution of a matrix equation.

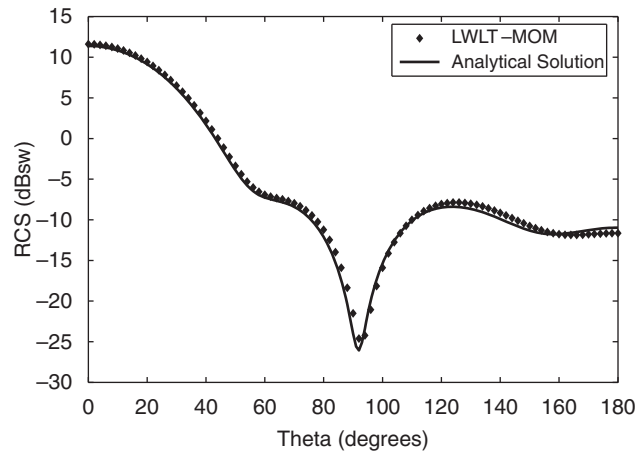


Figure 14. The E-plane RCS of a homogeneous dielectric sphere.

Table III. Sparsity of the wavelet-domain impedance matrix for 3-D objects and the CPU time consumed for the solution of the impedance matrix equation.

Examples	Sparsity (%)	MOM	LWLT-MOM	
		iteration time (s)	Time for wavelet matrix transform (s)	Iteration time (s)
Figure 11	34.81	38.4	2.4	15.86
Figure 12	33.04	51.8	1.9	16.72
Figure 13	26.8	62.5	4.8	18.43
Figure 14	32.8	61.7	5.7	24.18

As compared with the traditional wavelet matrix method, the proposed method is an in-place method, which can speedup the wavelet transform by a factor of two without the help of FFT, and can be applied to overcome the limitation in the matrix dimension.

Special issues such as the application of lifting wavelet packet transform to CEM, further improving the sparsity of impedance matrix, and the application of the proposed method to fast algorithms can be the topics for future work. In particular, owing to its generality in handling a matrix equation, the proposed technique can be extended to other engineering computation areas if there is a matrix equation, which will pave a broad way for the application of the WMT.

ACKNOWLEDGEMENTS

The authors wish to acknowledge the anonymous reviewers for their useful comments and constructive suggestions. This work is supported by Anhui Provincial Natural Science Foundation under Grant No. 090412047 and the Natural Science Foundation of the Anhui Higher Education Institution of China under Grant No. KJ2008A036, and partially by the National Natural Science Foundation of China (No.60671051).

REFERENCES

1. Harrington RF. *Field Computation by Moment Methods*. Macmillan: New York, 1968.
2. Rao SM, Wilton DR, Glisson AW. Electromagnetic scattering by surface of arbitrary shape. *IEEE Transactions on Antennas and Propagation* 1982; **30**:409–418.
3. Jin JM, Chew WC, Michielssen E, Song JM. *Fast and Efficient Algorithms in Computational Electromagnetics*. Artech House: Boston, 2001.
4. Tong MS. A stable integral equation solver for electromagnetic scattering by large scatterers with concave surface. *Progress in Electromagnetics Research* 2007; **74**:113–130.
5. Golik WL. Wavelet packets for fast solution of electromagnetic integral equations. *IEEE Transactions on Antennas and Propagation* 1998; **46**:618–624.
6. Rokhlin V. Rapid solution of integral equations of scattering theory in two dimensions. *Journal of Computational Physics* 1990; **86**:414–439.
7. Engheta N, Murphy WD, Rokhlin V, Vassiliou MS. The fast multipole method (FMM) for electromagnetic scattering problems. *IEEE Transactions on Antennas and Propagation* 1992; **40**:634–641.
8. Coifman R, Rokhlin V. The fast multipole method for the wave equation: a pedestrian prescription. *IEEE Antennas and Propagation Magazine* 1993; **35**:7–12.
9. Song JM, Chew WC. Multilevel fast-multipole algorithm for solving combined field integral-equations of electromagnetic scattering. *Microwave and Optical Technology Letters* 1995; **10**:14–19.
10. Lu WB, Cui TJ, Zhao H. Acceleration of fast multipole method for large-scale periodic structures with finite sizes using sub-entire-domain basis functions. *IEEE Transactions on Antennas and Propagation* 2007; **55**:414–421.
11. Bleszynski E, Bleszynski M, Jaroszewicz T. AIM: adaptive integral method for solving large-scale electromagnetic scattering and radiation problems. *Radio Science* 1996; **31**:1225–1251.
12. Sarkar TK, Arvas E, Rao SM. Application of FFT and the conjugate gradient method for the solution of electromagnetic radiation from electrically large and small conducting bodies. *IEEE Transactions on Antennas and Propagation* 1986; **34**:635–640.
13. Yung EKN, Chen RS, Tsang KF, Mo L. The block-Toeplitz-matrix-based CG-FFT algorithm with an inexact sparse preconditioner for analysis of microstrip circuits. *Microwave and Optical Technology Letters* 2002; **34**:347–351.
14. Steinberg ZB, Leviatan Y. On the use of wavelet expansions in the method of moments. *IEEE Transactions on Antennas and Propagation* 1993; **41**:610–619.
15. Wagner RL, Chew WC. A study of wavelets for the solution of electromagnetic integral-equations. *IEEE Transactions on Antennas and Propagation* 1995; **43**:802–810.
16. Wang G. Application of wavelets on the interval to numerical analysis of integral equations in electromagnetic scattering problems. *International Journal for Numerical Methods in Engineering* 1997; **40**:1–13.
17. Wang G. On the utilization of periodic wavelet expansions in the moment methods. *IEEE Transactions on Microwave Theory and Techniques* 1995; **43**:2495–2498.
18. Barmada S, Raugi M. Analysis of scattering problems by MOM with intervallic wavelets and operators. *Applied Computational Electromagnetics Society Journal* 2003; **18**:62–67.
19. Lashab M, Benabdelaziz F, Zebiri C. Analysis of electromagnetics scattering from reflector and cylindrical antennas using wavelet-based moment method. *Progress in Electromagnetics Research* 2007; **76**:357–368.
20. Su C, Sarkar TK. Multiscale moment method for solving Fredholm integral equation of the first kind-summary. *Journal of Electromagnetic Waves and Applications* 1998; **12**:97–101.
21. Sokolik D, Shifman Y, Leviatan Y. Improved impedance matrix compression (IMC) technique for efficient wavelet-based method of moments solution of scattering problems. *Microwave and Optical Technology Letters* 2004; **40**:275–280.
22. Golik WL. Sparsity and conditioning of impedance matrices obtained with semi-orthogonal and bi-orthogonal wavelet bases. *IEEE Transactions on Antennas and Propagation* 2000; **48**:473–481.
23. Sarkar TK, Wicks MC, Salazar-Palma M. *Wavelet Applications in Engineering Electromagnetics*. Artech House: London, 2002.
24. Deng H, Ling H. Moment matrix sparsification using adaptive wavelet packet transform. *Electronics Letters* 1997; **33**:1127–1128.
25. Pan GW, Tretiakov YV, Gilbert B. Smooth local cosine based Galerkin method for scattering problems. *IEEE Transactions on Antennas and Propagation* 2003; **51**:1177–1184.
26. Daubechies I, Sweldens W. Factoring wavelet transforms into lifting steps. *Journal of Fourier Analysis and Applications* 1998; **4**:247–269.